FULL PAPER

Dalton
www.rsc.org/dalton

C–H and C–C agostic interactions in cycloalkyl tris(pyrazolyl)boratoniobium complexes †

Joëlle Jaffart,[a] Marcus L. Cole,‡[a] Michel Etienne,*[a] Meike Reinhold,[b] John E. McGrady *[b] and Feliu Maseras *[c]

[a] *Laboratoire de Chimie de Coordination du CNRS, UPR 8241, 205 Route de Narbonne 31077, Toulouse, France. E-mail: etienne@lcc-toulouse.fr; Fax: +33 5 61 55 30 03; Tel: +33 5 61 33 31 76*

[b] *Department of Chemistry, University of York, York, UK YO10 5DD. E-mail: jem15@york.ac.uk; Fax: +44 1904 432516; Tel: +44 1904 434539*

[c] *Unitat de Quimica Fisica, Edifici Cn, Universitat Autonoma de Barcelona, 08193 Bellaterra, Catalonia, Spain. E-mail: feliu@klingon.uab.es; Fax: +34 93 5812920; Tel: +34 93 5812851*

Received 12th May 2003, Accepted 19th June 2003
First published as an Advance Article on the web 22nd September 2003

Cycloalkyl niobium complexes, $Tp^{Me2}NbX(R)(MeC{\equiv}CMe)$ (Tp^{Me2} = hydrotris(3,5-dimethylpyrazolyl)borate; X = Cl, R = *c*-C_3H_5 (**2a**); X = Br, R = *c*-C_3H_5 (**2b**), X = Cl, R = *c*-C_5H_9 (**3**), X = Cl, R = *c*-C_6H_{11} (**4**),) have been prepared from $Tp^{Me2}NbCl_2(MeC{\equiv}CMe)$. The cyclopropyl complex **2a** shows no sign of C–H agostic interactions either in the solid state (X-ray) or in solution. In contrast, the NMR spectra of **3** and **4** are temperature dependent as a consequence of an equilibrium between a major α-agostic species and a minor non-agostic one. Hybrid QM/MM calculations are used to rationalise the behaviour of these cycloalkyl species, and illustrate the subtle interplay of steric and electronic effects in these systems.

Introduction

The 'agostic' interaction beween transition metal centres and a C–H bond[1] remains a topic of enduring interest, and current research ranges from fundamental studies into the nature of the chemical bond to highly applied work examining the role of agostic bonds in catalysis.[2–12] In a series of recent papers,[13–19] we have described the synthesis of a series of alkyl complexes of niobium, $Tp^{Me2}NbX(R)(PhC{\equiv}CMe)$ and $Tp^{Me2}NbX(R)$-$(MeC{\equiv}CMe)$ (Tp^{Me2} = hydrotris(3,5-dimethylpyrazolyl)borate) (Fig. 1) and conducted detailed spectroscopic and theoretical investigations into the nature of the agostic interactions between the metal centre and the alkyl substituent. Our initial studies focussed on acyclic species, R = Et and *i*-Pr, where structural and spectroscopic data confirmed the presence of α-C–H agostic interactions. For the ethyl complex the α-agostic isomer is the only species present in solution, whereas in the isopropyl analogue, it is in equilibrium with its β-C–H agostic counterpart (one of the few examples of equilibria between two such isomeric agostic species).[20] The observation of α-C–H agostic bonds is in itself a rather uncommon phenomenon, and is usually restricted to systems where alternative β-C–H bonds are unavailable.[21,22] Previous studies have confirmed that β-agostic interactions are generally preferred on electronic grounds, and so the apparent preference for the α-agostic alternative in these systems prompted us to investigate the electronic structure of these systems using the hybrid QM/MM methodology that has emerged in recent years as an effective means of investigating electronic structure in transition metal organometallic systems.[23–26] Our initial investigations[17] indicated that the methyl groups in the 3-positions on the trispyrazolylborato ligand play a key role in this unusual chemistry by projecting down onto the opposite face of the octahedrally coordinated metal, and imposing a hindered coordination environment upon the alkyl ligand. The favoured orientation of the alkyl group in all cases is the one where the bulkiest substituent on the α carbon bisects two of these methyl groups, effectively directing it away from the metal centre. The 'agostic' site is then occupied by one of the two remaining less bulky substituents, both of which are hydrogen atoms in the case of R = Et. For the *i*-Pr species, one Me group occupies the wedge, and α and β agostic structures are observed when the remaing H and Me substituents, respectively, occupy the agostic site. In a later publication,[18] we extended these studies to the bulkier *sec*-Bu complex, and showed that similar principles could account for the more complex equilibria observed in this case. In particular, the presence of a chiral centre at the α carbon gave rise to two distinct diastereomers with very different agostic properties, the relative energies of which were again determined by the steric demands of the methyl groups.These fundamental studies have shed some light on some of the factors that control agostic bonding and, in particular, have highlighted the fact that the presence of unusual types of agostic bonding may be a result of steric factors which disfavour alternative structures rather than any intrinsically strong electronic driving force. In a very recent communication,[19] we turned our attention to the cyclopropyl species, $Tp^{Me2}NbCl(c\text{-}C_3H_5)(MeC{\equiv}CMe)$, where experiment and theory are consistent with the presence of a highly unusual agostic bond between the metal centre and a C–C, rather than C–H (either α or β) bond. To the best of our knowledge, only a very few examples of agostic C–C bonds have been proposed

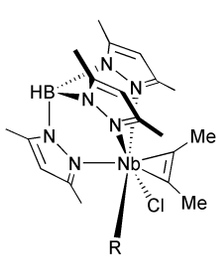

R = *c*-C_3H_5, *c*-C_5H_9, *c*-C_6H_{11}

Fig. 1 Hydridotris(pyrazolyl)borato cycloalkyl niobium complex.

† Based on the presentation given at Dalton Discussion No. 6, 9–11th September 2003, University of York, UK. Electronic supplementary information (ESI) available: A view of the unit cell for **3**. A variable-temperature ^1H NMR experiment for **3**. Cartesian coordinates and total energies of all optimised structures reported herein. See http://www.rsc.org/suppdata/dt/b3/b305296f/

‡ Present address: School of Chemistry, P.O Box 23, Monash University, Victoria 3800, Australia.

DOI: 10.1039/b305296f

previously in the literature, the majority occurring in cases where alternative C–H agostic structures are not accessible.[27–30] In the case of the rather compact cyclopropyl group, preliminary calculations indicate that the steric effects of the pendant methyl groups are less important, and the preference for the C–C agostic structure is instead determined by the unusual electronic properties of the small ring system. This observation serves to highlight the rich diversity of chemistry associated with such weak bonds, and also illustrates the potential for controlling the properties of a complex by rather subtle chemical modifications. In this contribution, we expand the chemistry of the cycloalkyl systems by reporting new data on the cyclopropyl systems and presenting a detailed study of analogous cyclopentyl and cyclohexyl species, $Tp^{Me2}NbCl(c\text{-}C_5H_9)(MeC{\equiv}CMe)$ and $Tp^{Me2}NbCl(c\text{-}C_6H_{11})(MeC{\equiv}CMe)$ (Fig. 1). The progression from C_3 to C_5 and C_6 ring systems represents an increase in the steric bulk, while at the same time alleviating the effects of strain within the ring system. In light of these competing factors, we anticipated that these new systems might exhibit diverse structural and solution chemistry based on the presence of a number of energetically close agostic isomers.

Experimental

All experiments were carried out under a dry dinitrogen atmosphere using either Schlenck tube or glove-box techniques. THF and diethyl ether were obtained after refluxing purple solutions of Na/benzophenone under dinitrogen. Toluene, hexane, pentane and 1,4-dioxane were dried by refluxing over CaH_2 under dinitrogen. Deuterated NMR solvents were dried over molecular sieves, degassed by freeze-pump-thaw cycles and stored under dinitrogen. Data are reported in dichloromethane-d_2 unless otherwise stated. ^1H and ^{13}C NMR spectra were obtained on Bruker DPX 300 and AMX 400 spectrometers. Only pertinent $^1J_{CH}$ are quoted in the ^{13}C spectra. COSY ^1H–^1H and HMQC ^{13}C–^1H spectra have occasionally been used to secure assignments (see text). Elemental analyses were performed in the Analytical Service of our Laboratory. $Tp^{Me2}NbCl_2(MeC{\equiv}CMe)$ (**1**) was prepared according to the published procedure.[31] Grignard reagents (RMgX in diethyl ether) were either purchased or synthesised *via* classical procedures.

Synthesis

Virtually the same procedure was used to prepared all the complexes. 1,4-Dioxane (2 mL) was added to a solution of $(c\text{-}C_3H_5)MgBr$ in diethyl ether (20 mL, 0.076 M, prepared from Mg turnings and $c\text{-}C_3H_5Br$ in diethyl ether) yielding an abundant precipitate. After decantation, 10 mL of this solution were added dropwise *via* syringe to a cooled (−20 °C, ethanol/liquid nitrogen bath) diethyl ether solution (30 mL) of **1** (0.250 g, 0.49 mmol). The colour of the solution changed gradually from purple–red to yellow–orange as the temperature rose slowly to room temperature. Stirring was maintained for *ca*. 1 h. The resulting slurry was filtered through a pad of Celite to give a clear yellow–orange solution which was evaporated to dryness. The residue was dissolved in a minimum amount of toluene (*ca*. 2 mL). Addition of hexane (*ca*. 10 mL) followed by paper filtration yielded orange crystals of $Tp^{Me2}NbCl(c\text{-}C_3H_5)(MeC{\equiv}CMe)$ (**2a**) (0 °C, overnight) which were collected by filtration, washed with small amounts of cold pentane and dried under vacuum (0.200 g, 0.39 mmol, 78%). For the synthesis of (**2b**), (**3**) and (**4**), the use of 1,4-dioxane was not necessary although it occasionally helps to precipitate MgX_2 salts.

$Tp^{Me2}NbCl(c\text{-}C_3H_5)(MeC{\equiv}CMe)$ (2a)

Anal. Calc. for $C_{22}H_{33}N_6BClNb$: C 50.84, H 6.35, N 16.18. Found: C 50.37, H 6.38, N 15.89%. ^1H NMR (300 MHz, benzene-d_6, 300 K): δ 5.73, 5.70, 5.46 (s, 1H each, Tp^{Me2} C*H*), 3.11, 2.18 (s, 3H each, *Me*C≡C*Me*), 2.82, 2.21, 2.10, 2.06, 2.03, 1.92 (s, 3H each, Tp^{Me2} *Me*), 2.24, 1.53, 1.26, 0.95 (m, 2, 1, 1, 1H each, respectively, CH_2β, CH_2β′ and C*H*α). ^{13}C NMR (75 MHz, benzene-d_6, 300 K): δ 243.8, 231.8 (Me*C*≡*C*Me), 153.3, 151.6, 144.0, 143.9, 143.8 (1, 2, 1, 1, 1, Tp^{Me2} *C*Me), 108.2, 107.8, 107.7 (Tp^{Me2} *C*H), 75.3 (d, $^1J_{CH}$ 139 Hz, $w_{1/2}$ = 20 Hz, *C*αH), 23.2, 13.8 (t each, $^1J_{CH}$ 159 Hz, *C*βH_2 and *C*β′H_2), 21.9, 20.8, 16.4, 15.8, 15.1, 13.2, 13.0, 12.7 (Tp^{Me2} C*Me* and *Me*C≡C*Me*).

$Tp^{Me2}NbBr(c\text{-}C_3H_5)(MeC{\equiv}CMe)$ (2b)

Anal. Calc. for $C_{22}H_{33}N_6BBrNb$: C 46.76, H 5.84, N 14.88. Found C 47.54, H 5.96, N 14.80%. ^1H NMR (300 MHz, benzene-d_6, 300 K): δ 5.76, 5.70, 5.46 (s, 1H each, Tp^{Me2} C*H*), 3.23, 2.15 (s, 3H each, *Me*C≡C*Me*), 2.85, 2.21, 2.10, 2.03, 2.02, 1.90 (s, 3H each, Tp^{Me2} *Me*), 2.34, 2.24, 1.49, 1.25, 0.87 (m, 1H each, CH_2β, CH_2β′ and C*H*α). ^{13}C NMR (75 MHz, benzene-d_6, 300 K): δ 245.7, 234.5 (Me*C*≡*C*Me), 153.7, 151.7, 151.6, 144.3, 144.1, 143.8 (Tp^{Me2} *C*Me), 108.4, 107.9, 107.8 (Tp^{Me2} *C*H), 79.3 (broad d, $^1J_{CH}$ = 139 Hz, $w_{1/2}$ = 15 Hz, *C*αH), 24.1, 13.7 (t each, $^1J_{CH}$ = 159 Hz, *C*βH_2 and *C*β′H_2), 22.3, 21.8, 17.3, 16.0, 15.9, 13.2, 13.0, 12.7 (Tp^{Me2} C*Me* and *Me*C≡C*Me*).

$Tp^{Me2}NbCl(c\text{-}C_5H_9)(MeC{\equiv}CMe)$ (3)

Anal. Calc. for $C_{24}H_{37}N_6BNbCl$: C 52.54, H 6.75, N 15.32. Found: C 51.82, H 6.31, N 15.43%. ^1H NMR (400 MHz): At 293 K): δ 5.94, 5.91, 5.75 (s, 1H each, Tp^{Me2} C*H*), 3.28, 2.32 (s, 3H each, *Me*C≡C*Me*), 2.53, 2.49, 2.46, 2.38, 1.91, 1.78 (s, 3H each, Tp^{Me2} *Me*), 2.93, 2.14 (pseudo-sextet, 1H each, $^3J_{HH}$ = 7 Hz, C*H*β′), 1.61 (dddd, 1H, $^2J_{HH}$ = 14 Hz, $^3J_{HH}$ = 3, 7 and 10 Hz, CHβ), 1.33 (pseudo-quintet, 2H, $^3J_{HH}$ = 7 Hz, C*H*γ′), 1.14–1.06 (m, 1H, C*H*γ), 1.00–0.90 (m, 1H, C*H*γ), 0.52 (pseudo-septet, 1H, $^3J_{HH}$ = 7 Hz, C*H*β), −0.39 (quintet, 1H, $^3J_{HH}$ = 6.9 Hz, C*H*α). At 193 K: δ 5.91, 5.90, 5.76 (s, 1H each, Tp^{Me2} C*H*), 3.23, 2.22 (s, 3H each, *Me*C≡C*Me*), 2.42, 2.41, 2.39, 2.32, 1.79, 1.67 (s, 3H each, Tp^{Me2} *Me*), 3.04 (1H, C*H*β′), 2.16 (partially obscured, 1H, C*H*β′), 1.49 (1H, C*H*β), 1.30, 1.13 (1H each, C*H*γ′), 1.02, 0.74 (1H each, C*H*γ), 0.24 (1H, C*H*β), −0.93 (NbC*H*). ^{13}C NMR (100 MHz, 193 K): δ 244.5, 222.2 (Me*C*≡*C*Me), 151.3, 150.7, 150.2, 144.5, 144.4, 143.9 (Tp^{Me2} *C*Me), 135.8 (d, $^1J_{CH}$ = 93 Hz, $w_{1/2}$ = 8 Hz, NbC*H*), 107.1, 106.5, 106.2 (Tp^{Me2} C*H*), 40.6, 39.1 (t, $^1J_{CH}$ = 127 Hz, *C*β′H_2, *C*βH_2, respectively), 27.5, 27.3 (t, $^1J_{CH}$ = 127 Hz, *C*γH_2, *C*γ′H_2), 21.7, 21.4, 14.4, 13.9, 13.8, 13.1, 12.8, 12.6 (q, 127 Hz, Tp^{Me2} *C*H_3 and *Me*C≡C*Me*). ^{13}C NMR (62.6 MHz, benzene-d_6, 293 K): δ 245.5, 224.3 (Me*C*≡*C*Me), 152.6, 151.5, 146.6, 143.8 (3, 3, 6, 6 resp., Tp^{Me2} *C*Me), 125.6 (d, $^1J_{CH}$ = 102 Hz, $w_{1/2}$ = 17 Hz, Nb*C*H), 108.3, 107.6, 107.4 (Tp^{Me2} *C*H), 40.4, 38.2, 28.6, 28.0 (all t, $^1J_{CH}$ = 129 Hz, *C*β′H_2, *C*βH_2, *C*γH_2, *C*γ′H_2), 22.1, 21.7, 15.5, 14.9, 14.6, 13.1, 12.8, 12.5 (Tp^{Me2} *C*H_3 and *Me*C≡C*Me*).

$Tp^{Me2}NbCl(c\text{-}C_6H_{11})(MeC{\equiv}CMe)$ (4)

Anal. Calc. for $C_{25}H_{39}N_6ClBNb$: C 53.36, H 6.99, N 14.94. Found: C 53.76, 7.31, 14.83%. ^1H NMR (400 MHz) 293 K: δ 5.95, 5.92, 5.71 (s, 1H each, Tp^{Me2} C*H*), 3.18, 2.25 (s, 3H each, *Me*C≡C*Me*), 2.67, 2.48, 2.46, 2.34, 2.00, 1.72 (all s, 3H each, Tp^{Me2} C*Me*), 2.30, 1.60–1.45, 1.40–1.25, 1.05–0.90, 0.70–0.55 (m, 1, 3, 3, 2, 1H each, CH_2β, CH_2β′, CH_2γ, CH_2γ′, C*H*δ), 0.15 (broad s, 1H, C*H*α). At 193 K: major species **4**: δ 5.98, 5.97, 5.75 (s, 1H each, Tp^{Me2} C*H*), 3.20, 2.16 (s, 3H each, *Me*C≡C*Me*), 2.54, 2.39, 2.38, 2.26, 1.93, 1.56 (s, 1H each, Tp^{Me2} C*Me*), 2.77 (m, 1H, C*H*β_{ax}), 1.65 (m, 1H, C*H*β_{eq}), 1.40 (m, 1H, C*H*γ_{ax}), 1.30 (m, 1H, C*H*δ_{ax}), 1.18 (m, 1H, C*H*β′$_{ax}$), 1.13 (m, 1H, C*H*γ′$_{ax}$), 1.02 (m, 1H, C*H*γ_{eq}), 0.82 (m, 1H, C*H*δ_{eq}), 0.75 (m, 1H, C*H*γ′$_{eq}$), 0.12 (m, 1H, C*H*β′$_{eq}$), −1.00 (m, 1H, NbC*H*α); minor species **4′** (several signals obscured): 5.94, 5.90, 5.81 (s, 1H each,

Tp^{Me2} C*H*), 3.16 (s, 3H, *Me*C≡), 2.69, 2.24, 1.79 (s, Tp^{Me2} C*Me*), 2.25 (m, NbC*Hα*). Rotamer ratio **4** : **4′** = 11 : 1. ^{13}C NMR (100 MHz, 193 K): major species **4**: δ 244.2, 227.2 (Me*C*≡*C*Me), 151.1, 150.4, 150.1, 144.5, 144.4, 144.1 (Tp^{Me2} *C*Me), 130.3 (d, $^1J_{CH}$ = 94 Hz, $w_{1/2}$ = 17 Hz, Nb*C*H), 109.3, 107.2 (1 : 2 resp., Tp^{Me2} *C*H), 41.9, 37.8, 31.6, 30.1, 27.2 (all t, $^1J_{CH}$ = 127 Hz, $w_{1/2}$ = 13 Hz, *C*β, *C*β′, *C*γ, *C*γ′, *C*δ resp.), 22.8, 22.7 (≡C*C*H_3), 16.0, 15.9, 14.8, 14.2, 13.9, 13.6 (Tp^{Me2} CH_3); minor species **4′** (several signals obscured): δ 224.2, 234.0 (Me*C*≡*C*Me), 153.0, 151.8, 149.0, 144.9 (Tp^{Me2} *C*Me), 109.4, 108.0, 107.5 (Tp^{Me2} *C*H), 93.8 (d, $^1J_{CH}$ = 120 Hz, Nb*C*H).

Crystallographic studies

X-Ray crystal structures of **2a** and **2b** were previously reported (see CCDC 201292 and 201293).[19] Single crystals of **3** were obtained from toluene–pentane mixtures. The data collection (T = 160 K) was performed on a STOE IPDS diffractometer using graphite-monochromatised Mo-Kα radiation. The structure was solved by direct methods using SIR92.[32] The refinement was carried out with the CRYSTALS package.[33] All atoms, except hydrogens and those of a solvent molecule (0.5 toluene molecule in the asymmetric unit), were anisotropically refined. Except for H(1) and H(11), which were observed in a difference Fourier map and subsequently refined with a fixed isotropic thermal parameter, all hydrogen atoms were included in the calculation in idealised positions (C–H = 0.96 Å) with an isotropic thermal parameter 1.2 times that of the atom to which they were attached. No absorption corrections were made. In the asymmetric unit for **3**, half a molecule of toluene is disordered around the inversion center (see ESI †). Full-matrix least-square refinements were carried out by minimizing the function $\Sigma w(||F_o| - ||F_c|)^2$, where F_o and F_c are the observed and calculated structure factors. A weighting scheme was introduced with $w = w'[1 - (\Delta F/6\sigma(F))^2]^2$.[34] The model reached convergence with $R = \Sigma(||F_o| - ||F_c|)/\Sigma|F_o|$, $R_w = [\Sigma w(||F_o| - ||F_c|)^2/\Sigma w(|F_o|)^2]^{1/2}$ having values of 0.0340 and 0.0349. Plots of molecular structures (for **2a**, Fig. 2; for **3**, Fig. 3) were performed by using the software CAMERON.[35]

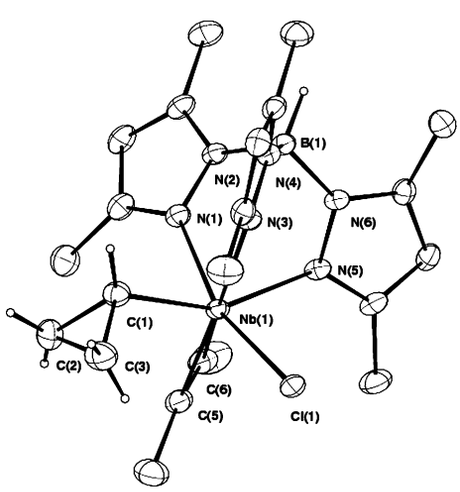

Fig. 2 Plot of the molecular structure of Tp^{Me2}NbCl(*c*-C_3H_5)(MeC≡CMe).

For **3**: $C_{24}H_{37}NbClN_6B\cdot0.5C_7H_8$, M = 594.84, monoclinic, $C2/c$, a = 39.571(5), b = 13.711(1), c = 10.669(1) Å, β = 96.52(2)°, V = 5751(1) Å^3, Z = 8, T = 160 K, μ = 5.4 cm^{-1}, 16617 measured reflections, 3734 independent reflections (R_{int} = 0.0432), final R = 0.0277 (on F), R_w = 0.0346 for 2705 reflections with $I > 2\sigma(I)$ and 351 parameters.

CCDC reference number 210405.

See http://www.rsc.org/suppdata/dt/b3/b305296f/ for crystallographic data in CIF or other electronic format.

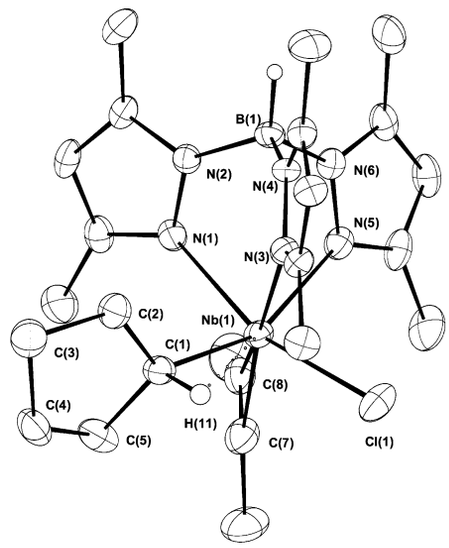

Fig. 3 Plot of the molecular structure of Tp^{Me2}NbCl(*c*-C_5H_9)(MeC≡CMe).

Computational details

All calculations were carried out with the ONIOM method[23,24] as implemented in the Gaussian98 package.[36] The quantum mechanical (QM) part was defined by $[Nb(NH{=}CH_2)_3(Cl)(HC{\equiv}CH)(R)]^+$, the full alkyl group involved in the agostic interaction being therefore included in the QM region. This type of partition of Tp^{Me2} ligands has been proved satisfactory in previous calculations by our group.[17–19,37] The method applied for the QM region was Becke3LYP.[38,39] An effective core potential was used to replace the 36 innermost electrons of niobium[40] and the 10 innermost electrons of chlorine.[41] The valence double zeta basis set associated with the pseudopotential in the program[36] was used for niobium and chlorine, supplemented with a d shell in the latter case.[42] The 6-31g(d) basis set[43] was used for all atoms of the alkyne and alkyl ligands, as well as for the nitrogen atoms of Tp^{Me2}. The 6-31g basis set[44] was used for the rest of the atoms of Tp^{Me2} in the QM partition. The force field used for the molecular mechanics (MM) partition was UFF,[45] as implemented in the program.[36] All geometry optimizations were full, with no restrictions, unless indicated explicitly in the text.

Results and discussion

Syntheses

Treatment of a red–purple diethyl ether solution of the dichloroniobium complex[31] $Tp^{Me2}NbCl_2$(MeC≡CMe) (**1**) with one equivalent of the appropriate chloro or bromo alkyl Grignard reagent at low temperature (−20 °C) gives orange crystals of Tp^{Me2}NbX(R)(MeC≡CMe) (X = Cl, R = *c*-C_3H_5 (**2a**), X = Br, R = *c*-C_3H_5 (**2b**); X = Cl, R = *c*-C_5H_{11} (**3**), X = Cl, R = *c*-C_6H_{11} (**4**)) in good yield (*ca.* 75%). **2a** can be obtained selectively using a diethyl ether solution of (*c*-$C_3H_5)_2$Mg(dioxane)$_n$. Under strict exclusion of air, the colour of the reaction mixture of **3** darkens and occasionally turns violet rapidly. This violet solution leads to decomposition of the complex (^{1}H NMR). This colour changes is not observed in the case of the cyclopropyl and cyclopentyl complexes (**2a**, **2b**, **3**). This phenomenon leads to the *in situ* isomerization of the secondary alkyl complexes to their *n*-alkyl analogues.[18]

Cyclopropyl complexes, Tp^{Me2}NbCl(*c*-C_3H_5)(MeC≡CMe) and Tp^{Me2}NbBr(*c*-C_3H_5)(MeC≡CMe) (2a,2b)

As reported in a previous communication,[19] the crystal structures of the two cyclopropyl complexes show no evidence of

Table 1 Selected bond distances, angles and torsion angles for $Tp^{Me2}NbCl(c\text{-}C_3H_5)(MeC{\equiv}CMe)$ (**2a**)

Bond length/Å		Bond angle/°		Torsion angle/°	
Nb(1)–Cl(1)	2.4465(6)	Cl(1)–Nb(1)–C(1)	110.85(8)	Cl(1)–Nb(1)–C(1)–C(3)	24
Nb(1)–C(1)	2.159(3)	Nb(1)–C(1)–C(2)	131.4(2)	N(5)–Nb(1)–C(1)–C(2)	142
Nb(1) ··· H(11)	2.72(4)	Nb(1)–C(1)–C(3)	109.7(2)	Cl(1)–Nb(1)–C(1)–H(11)	104
C(1)–C(3)	1.539(4)	Nb(1)–C(1)–H(11)	115.2(20)		
C(2)–C(3)	1.478(5)	C(1)–C(2)–C(3)	62.5(2)		
C(1)–C(2)	1.490(4)	C(1)–C(3)–C(2)	59.1(2)		
Nb(1) ··· C(3)	3.045(3)	C(2)–C(1)–C(3)	58.4(2)		

agostic C–H interactions, either α or β (Fig. 2, Table 1). The orientation of the cyclopropyl group is such that the located α-hydrogen lies 2.72(4) Å from the metal centre, effectively precluding any significant agostic interaction. Although the β-hydrogens were not located, the rather large Nb–Cα–Cβ angles of 109.7(2) and 131.4(2)° are also inconsistent with the narrow angles usually associated with a β-agostic interaction. Nevertheless, the Nb(1)–C(1) bond of 2.159(3) Å is among the shortest we have ever seen in our series of either α- or β-agostic alkyl complexes of niobium(III) – the corresponding value in the acyclic analogue, $Tp^{Me2}NbCl(i\text{-}Pr)(PhC{\equiv}CMe)$ is 2.228(4) Å.[17,18] The Nb–Cl bond length in **2a** is 2.4465(6) Å, somewhat shorter than that in $Tp^{Me2}NbCl(i\text{-}Pr)(PhC{\equiv}CMe)$ (2.493(1) Å), consistent with the absence of a C–H agostic interaction. However, in previous papers we have emphasised the importance of the Cl–Nb–Cα bond angle as a structural indicator of agostic interactions, and the value of 110.85(8)° in **2a** is still much greater than 90°, albeit not as large as the 122.1(1)° observed in the β-agostic isopropyl derivative. Thus whilst the first coordination sphere of the metal centre appears to have rearranged to accommodate an additional electron pair, there appears to be no structural evidence that this pair comes from a C–H bond. The structure of the C_3 ring provides an alternative explanation, because one of the C–C bonds (C(1)–C(3)) is notably elongated relative to the other two. The degree of elongation (0.049 Å) is of the same order of magnitude as that observed for C–H bonds in neutron diffraction studies of agostic compounds. In $Tp^{Me2}RhCl(c\text{-}C_3H_5)(CN^tBu)$, where the 18-electron configuration effectively precludes agostic interactions the three C–C bonds are identical within experimental error [1.48(1), 1.49(1), 1.45(1) Å].[46a] Similar parameters are observed for the related $Cp^*RhBr(c\text{-}C_3H_5)(PMe_3)$.[46b] The elongation of a single bond also contrasts markedly with the contraction usually observed for β-C–H agostic systems, suggesting that it is the α-C–C bond, rather than one of the C–H bonds, that is interacting in an agostic fashion.

The ^1H NMR spectra of the cyclopropyl complexes **2a** and **2b** are temperature independent, and are entirely consistent with the conclusions drawn above. All of the cyclopropyl protons resonate as complex multiplets between δ 0.95 and 2.24 for **2a** and δ 0.87 and 2.34 for **2b**. We tentatively assign the shielded signal to Hα. ^{13}C NMR spectra show a doublet ($^1J_{CH}$ 139 Hz) for Cα at δ 75.3 and 79.3 for **2a** and **2b**, respectively. Cβ give triplets at δ 23.2 and 13.8 (**2a**) and δ 24.1 and 13.1 (**2b**) ($^1J_{CH}$ 159 Hz). These values are typical of cyclopropyl carbons, where sp^2 character is high.[47] Even though Cα is slightly deshielded (see below) and its $^1J_{CH}$ is reduced as compared to those for Cβ, no agostic interaction is apparent from the data. Similar $^1J_{CH}$ values (131 and 161 Hz for Cα and Cβ, respectively) have been observed for $(^tBu_3SiNH)_3Zr(c\text{-}C_3H_5)$.[48a,8] Even when ^{13}C NMR data are reported for early transition metal cyclopropyl complexes, $^1J_{CH}$ are rarely quoted. Cα resonates at δ 34.9 for $(^tBu_3SiNH)_3Zr(c\text{-}C_3H_5)$[48a] and at δ 57.9 for the related Ti complex $(^tBu_3SiO)_2(^tBu_3SiNH)Ti(c\text{-}C_3H_5)$.[48b]

Cyclopentyl complex, $Tp^{Me2}NbCl(c\text{-}C_5H_9)(MeC{\equiv}CMe)$ (3)

The crystal structure of the cyclopentyl complex (**3**) at 160 K (Fig. 3, Table 2) clearly reveals the presence of an α-C–H agostic interaction, with a short Nb–Cα bond of 2.174(4) Å. The located and refined α-agostic hydrogen lies in the Cl–Nb–C(α) plane at a distance of 2.21 Å from the metal centre, with a highly acute Nb–Cα–H angle of 79.9(24)°. The Nb–Cα–Cβ angles, in contrast, are slightly opened to accommodate this interaction. The C–C bond lengths, in contrast, are unremarkable, and show no sign of C–C agostic interactions. The overall orientation of the cyclopentyl ligand is such that it lies in a wedge formed by two pyrazolyl groups, placing both β carbons away from the pendant 3-methyl groups of Tp^{Me2} to minimise steric repulsions. The cyclopentyl group adopts an envelope conformation (see torsion angles, Table 2) with C(4) constituting the flap. The structure is very similar to that of $Cp_2ZrCl(c\text{-}C_5H_9)$,[49] except for absence of an agostic interaction in the latter.

Complex **3** exhibits dynamic NMR behavior, and assignment of the cyclic protons and carbons relies on ^1H–^1H and ^1H–^{13}C HMQC NMR data (see experimental section). The nine cyclopentyl ring protons give eight signals showing fine structure at 293 K in dichloromethane-d_2. When the temperature decreases (see ESI †), the signals broaden then sharpen again around 203 K. No splitting is observed and the fine structure due to J_{HH} couplings, although hardly measurable, is maintained at 193 K. The shielded α-H shifts from δ −0.39 (quintet, $^3J_{HH}$ = 6.9 Hz) at 293 K to δ −0.93 at 193 K. In the ^{13}C spectrum at 193 K, the niobium-bound carbon resonates as a remarkably deshielded doublet at δ 135.8 with a reduced coupling constant of $^1J_{CH}$ = 93 Hz. This signal is shifted to low field compared to the room-temperature spectrum (benzene-d_6, δ 125.6, d, $^1J_{CH}$ = 102 Hz). Not only do the data confirm an α-agostic interaction for **3**, they also suggest that there exists a process equilibrating a vastly major α-agostic form **3** with another non-α-agostic minor isomer **3′**. Analysis of the temperature dependent NMR spectra for **4** (see later) confirms this view.

Cyclohexyl complex, $Tp^{Me2}NbCl(c\text{-}C_6H_{11})(MeC{\equiv}CMe)$ (4)

No structural data are available for the cyclohexyl species (**4**), but a typical variable-temperature ^1H NMR experiment for **4** is shown Fig. 4. The figure shows a dynamic process equilibrating two distinct species namely **4** and **4′**, observable in the slow exchange limiting spectra in a 11 : 1 ratio. **4** clearly has an α-agostic interaction characterised at 183 K by a shielded ^1H NMR signal at δ −1.00 for NbCHα and a ^{13}C NMR doublet at δ 130.3 with a reduced $^1J_{CH}$ of 94 Hz for NbCHα. Characterization of **4′** is more difficult due to the low intensity and the complexity of the signals. However, a conspicuous ^{13}C NMR doublet at δ 93.8 ($^1J_{CH}$ = 120 Hz) assigned to Nb*C*Hα correlates (HMQC ^{13}C–^1H) with a ^1H NMR signal at δ 2.25 for Nb*C*Hα. The $^1J_{CH}$ is only slightly reduced compared to others within the cyclohexyl ring (127 Hz) giving evidence for a non-α-agostic NbCH. In the case of the isopropyl complex $Tp^{Me2}NbCl(i\text{-}Pr)(PhC{\equiv}CMe)$,[18] the α-carbon of the α-agostic rotamer resonates as a doublet centered at δ 126.4 with a $^1J_{CH}$ of 100 Hz, whereas the α-carbon of the β-agostic rotamer resonates as a doublet centered at δ 72.0 with a $^1J_{CH}$ of 141 Hz. Although definitive spectroscopic evidence for agostic interactions resides in a low $^1J_{CH}$, which is not observed in **4′**, it is interesting to note a deshielded Nb*C*Hα in the ^{13}C NMR spectra in our series of

Table 2 Selected bond distances, angles and torsion angles for $Tp^{Me2}NbCl(c\text{-}C_5H_9)(MeC{\equiv}CMe)$ (**3**)

Bond length/Å		Bond angle/°		Torsion angle/°	
Nb(1)–Cl(1)	2.430(1)	Cl(1)–Nb(1)–C(1)	108.9(1)	C(1)–C(2)–C(3)–C(4)	29
Nb(1)–C(1)	2.174(4)	Nb(1)–C(1)–C(2)	121.8(3)	C(2)–C(3)–C(4)–C(5)	41
Nb(1) ··· H(11)	2.21(4)	Nb(1)–C(1)–C(5)	127.5(3)	C(3)–C(4)–C(5)–C(1)	37
C(1)–C(2)	1.544(6)	Nb(1)–C(1)–H(11)	79.9(24)	C(4)–C(5)–C(1)–C(2)	19
C(2)–C(3)	1.523(6)	C(2)–C(1)–C(5)	104.4(4)	C(5)–C(1)–C(2)–C(3)	6
C(1)–C(5)	1.540(6)	C(1)–C(2)–C(3)	106.5(3)	Nb(1)–C(1)–C(2)–C(5)	154
		C(1)–C(5)–C(3)	105.7(4)	N(5)–Nb(1)–C(1)–C(2)	11
		C(2)–C(3)–C(4)	103.6(4)	N(5)–Nb(1)–C(1)–C(5)	137
				Cl(1)–Nb(1)–C(1)–H(11)	8

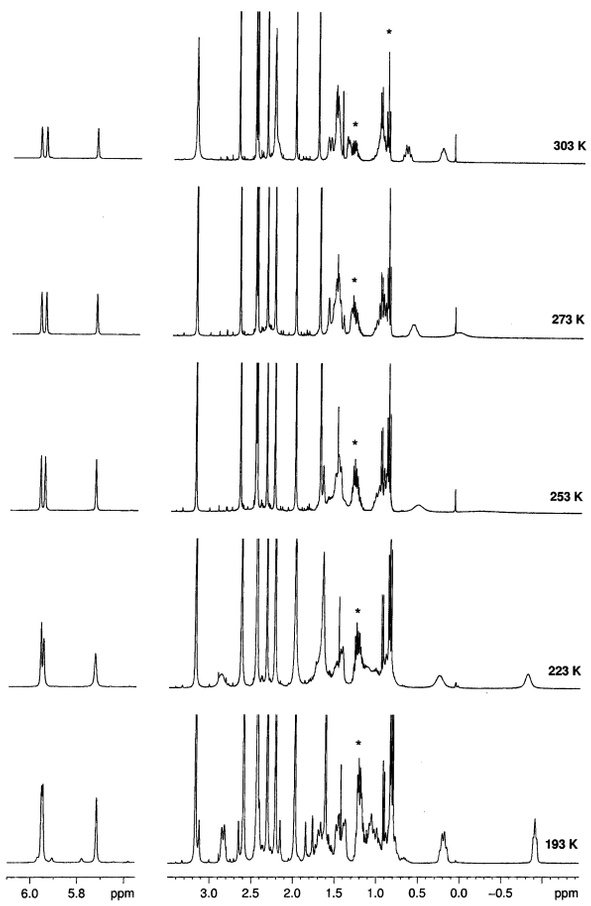

Fig. 4 Variable-temperature ^1H NMR spectrum (400 MHz, dichloromethane-d_2) of $Tp^{Me2}NbCl(c\text{-}C_6H_{11})(MeC{\equiv}CMe)$ (**3**) (* = residual pentane).

$Tp^{Me2}NbCl(R)(PhC{\equiv}CMe)$ (R = an α-agostic alkyl). Nb*C*Hα chemical shifts range from δ 86.5 (R = Et) and δ 95.9 (R = *n*-Pr)[15] to δ 126.4 (R = *i*-Pr)[18] and δ 135.8 (R = $c\text{-}C_5H_9$). Similar deshielded Cα are observed for the α-agostic $CpNbX(CH_2\text{-}t\text{Bu})_2(=N\text{-}2,6\text{-}C_6H_3\text{-}i\text{-}Pr_2)$ [X = Cl (δ 86.3), CH_2tBu (δ 85.7)],[50] whereas the non-agostic Nb*C*Hα resonates at higher field in the 18e complexes $Cp_2Nb(Et)(C_2H_4)$ (δ 11.2, $^1J_{CH}$ = 122 Hz),[51] and $Cp_2Nb(Et)(MeC{\equiv}CH)$ (δ 13.8, $^1J_{CH}$ = 135, 140 Hz).[52] Hence caution must be exercised when interpreting ^{13}C NMR chemical shifts. The 11 : 1 ratio between **4** and **4′** translates to ΔG°_{183} = −3.8 kJ mol^{-1}. Through a tentative assignment of a coalescence temperature of 248 K for the two Hα NMR signals ($\Delta\nu$ = 1255 Hz), an activation barrier, $\Delta G^\ddagger_{248}$, for this process can be estimated in the range 45–50 kJ mol^{-1}.[53]

Closely related equilibria between α- and β-agostic species have been observed in $Tp^{Me2}NbCl(i\text{-}Pr)(PhC{\equiv}CMe)$ and $Tp^{Me2}NbCl(sec\text{-}Bu)(MeC{\equiv}CMe)$ *via* coalescence techniques, and a similar barrier of 47.5 kJ mol^{-1} was measured for the former.[18] Direct observation of the dynamics of agostic interactions in alkyl complexes has been largely confined to β-agostic interactions. A windshield wiper motion has been shown to exchange the two α-agostic sites in $CpNb(CH_2\text{-}t\text{Bu})_2(=Nt\text{–Bu})$,[50] and hindered rotation about the Cr–C bond in $[Li(thf)_2]_2[Cr_2(CH_2SiMe_3)_6]$ also involves an α-agostic interaction.[54] A detailed study of equilibria between α- and β-agostic rotamers in $Cp^*_2YCH_2CH_2CH(CH_3)_2$ and related complexes has also appeared very recently.[20b] Isotopic perturbation of resonance (IPR) NMR studies have been used to probe similar phenomena in a range of tantalum complexes.[20a,55,56]

Computational analysis

In our previous papers, we have analysed the agostic bonding in these systems in terms of the structures and relative energies of three distinct rotamers, differing in their orientation about the Nb–C bond. Successive rotations of approximately 120° about this bond place the three different substituents on the α carbon in the 'agostic' site, bisecting the Cα–Nb–Cl angle (Scheme 1).

Optimised structural parameters and relative energies for the three rotamers are summarised in Table 3 (R = $c\text{-}C_3H_5$ and $c\text{-}C_5H_9$). The first point to note from the Tables is that the hybrid DFT/MM methodology accurately reproduces the experimental trends discussed in the previous section. For the cyclopropyl system, the most stable rotamer is A, where the C(1)–C(3) bond is in the agostic site, while B and C lie significantly higher in energy, consistent with the temperature independence of the NMR spectrum. The structural characteristics of **2a** are also well reproduced, most notably the long C(1)–C(3) bond (calc: 1.55 Å, X-ray: 1.539(4) Å). The optimised parameters for rotamers B and C also confirm that an agostic interaction occurs between the metal centre and whichever substituent happens to lie in the agostic site, leading to elongation of C(1)–H(11) (B) and C(1)–C(2) (C). For the cyclopentyl system, the relative energies of rotamers A and B are reversed, and the latter, where the α-C–H bond lies in the agostic site, is the most stable. The elongation of this bond (1.12 Å) is consistent with the presence of an α-C–H bond, as observed experimentally. On the basis of the calculated energies, we propose that rotamer A is the most likely candidate for the minor isomer observed in solution, **3′**. It is interesting to note that the two rotamers observed in solution are B (major) and A (major), whereas for the isopropyl system, they were B (minor) and C (major). Thus it appears that rotamer C is strongly destabilised relative to A in the cyclopentyl system. We return to this point in the following section.

The previous paragraph has shown that the ONIOM methodology is able to reproduce the extremely subtle balance between steric and electronic factors across the entire range alkyl substituents, both cyclic and acyclic. In order to identify the *origin* of these trends, however, we need to conduct a series of additional computational 'experiments' that allow us to separate the different factors involved. In particular, we aim to answer the following questions: (1) why is rotamer A the most stable for the cyclopropyl system, **2a**, but the least stable for the corresponding acyclic isopropyl? (2) why is an α-agostic C–C interaction preferred over a β-agostic C–H in rotamer A for **2a**

Table 3 Optimised structural parameters and relative energies of rotamers A, B and C for LNbCl(R)(MeC≡CMe), R = *c*-C_3H_5, *c*-C_5H_9

		L = Tp^{Me2}			L = $Tp^{5\text{-}Me}$		
		A	B	C	A	B	C
R = *c*-C_3H_5	Nb–C(1)/Å	2.16	2.16	2.18	2.16	2.17	2.17
	C(1)–C(2)/Å	1.51	1.51	1.53	1.51	1.51	1.54
	C(1)–C(3)/Å	1.55	1.51	1.52	1.54	1.50	1.06
	C(1)–H(11)/Å	1.09	1.11	1.09	1.09	1.11	1.09
	C(3)–C(1)–Nb–Cl/°	330	208	66	329	210	69
	Energy/kJ mol^{-1}	0	26	34	0	15	12
R = *c*-C_5H_9	Nb–C(1)/Å	2.21	2.20	2.22	2.21	2.20	2.22
	C(1)–C(2)/Å	1.54	1.54	1.57	1.56	1.56	1.56
	C(1)–C(5)/Å	1.57	1.54	1.54	1.56	1.55	1.55
	C(1)–H(11)/Å	1.10	1.12	1.09	1.10	1.12	1.09
	C(5)–C(1)–Nb–Cl/°	334	264	101	348	245	101
	Energy/kJ mol^{-1}	9	0	24	0	3	4

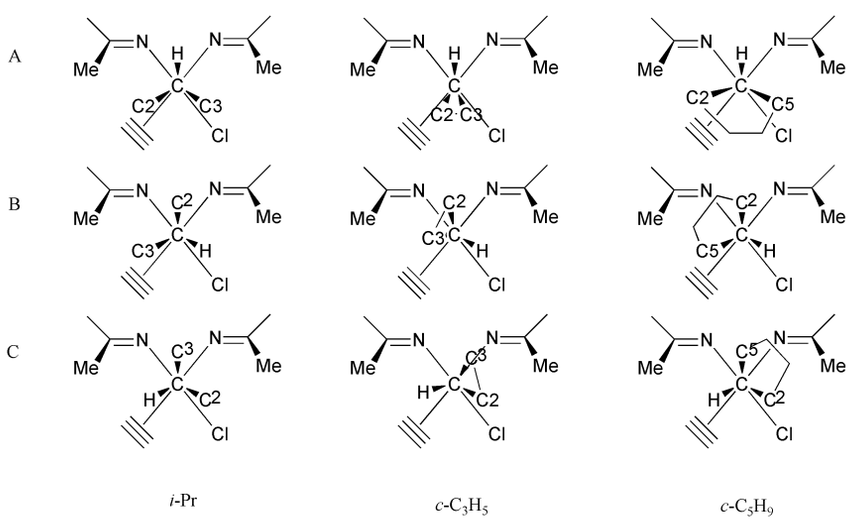

Scheme 1 Conformation of rotamers A, B and C in Tp^{Me2}NbCl(R)(MeC≡CMe), R = *i*-Pr, *c*-C_3H_5 and *c*-C_5H_9.

and **2b**? (3) why is rotamer C (β-C–H agostic) so strongly destabilised relative to B in the cyclopentyl complex. As a first step towards addressing these problems, each of the three rotamers was reoptimised using the modified ligand $Tp^{5\text{-}Me}$, which differs from Tp^{Me2} only in the absence of the methyl groups in the 3 position. We have shown previously that this modification relieves the steric pressure on the coordinated alkyl ligand, allowing electronic effects to dominate the position of the equilibrium between rotamers. Optimised geometries for the cyclopropyl and cyclopentyl complexes of $Tp^{5\text{-}Me}$ are also summarised in Table 3. In the cyclopropyl system, the removal of the pendant methyl groups does not change the identity of the most stable rotamer (A), but does stabilise the other two isomers relative to the ground state. This observation provides an interesting contrast with the acyclic species, where precisely the opposite effect was observed: the removal of steric bulk *stabilises* A relative to B and C. The difference between the isopropyl and cyclopropyl systems can be rationalised by comparing the nature of the steric interactions in the two cases (Scheme 1, *i*-Pr *vs.* *c*-C_3H_5). As noted previously, the least hindered site is the one bisecting the two nitrogen atoms, and as a result, rotamers B and C, where a methyl group occupies this position, are strongly favoured in the acyclic systems. In the cyclopropyl case, however, the acute C(2)–C(1)–C(3) angle draws C(2) and C(3) towards the methyl groups in the 3 positions in rotamers B and C, magnifying the steric clash. In complete contrast, in rotamer A the acute angle draws C(2) and C(3) away from the pendant methyl groups, reducing the steric effects. Whilst these rather subtle effects are of importance in developing our understanding of the systems as a whole, the most significant feature for the cyclopropyl system is the fact that steric effects do *not* determine the identity of the most stable isomer – rotamer A, the C–C agostic case, is preferred in both cases indicating that the origin of this preference must be electronic. The most obvious differences between the cyclopropyl ligand and its acyclic counterpart are the acute C–C–C bond angles, as a result of which the environment about each carbon is far from tetrahedral. We have therefore chosen to reinvestigate the ethyl complex (the simplest example where both α- and β-agostic isomers are accessible) but with the bond angles and torsions of the ethyl group constrained to replicate those in cyclopropane (fixed parameters taken from a calculation on cyclopropane with the same method: Nb–C(1)–H(11) = 114°, H(11)–C(1)–C(3) = 118°, H(11)–C(1)–H(2) = 118°, C(3)–C(1)–H(11)–Nb = −146°, H(2)–C(1)–H(11)–Nb = 146°). Optimised geometries and relative stabilities for this constrained ethyl system are compared to the corresponding system where the ethyl ligand is allowed to optimise freely in Table 4.

In the constrained system, only two rotamers, A and C, could be located; all attempts to find a minimum for rotamer B led instead to C. Most importantly, rotamer A, which is the least stable for freely optimised ethyl complex, is strongly stabilised, and is now the most stable by 21 kJ mol^{-1}, confirming that the highly distorted environment around the carbons in cyclopropane imposes a strong preference for rotamer A. The relative weakness of the C–C bonds in cyclopropane, caused by poor orbital overlap, is well established, and by constraining the angles and dihedrals about the α carbon, we have effectively imposed this instability on the ethyl group. The highly

Table 4 Comparison of optimised structural parameters and relative energies of $Tp^{Me2}NbCl(C_2H_5)(MeC{\equiv}CMe)$ for free and constrained optimisation

	Unconstrained			Constrained		
	A	B	C	A	B	C
Nb–C(1)/Å	2.22	2.18	2.22	2.14	–	2.18
C(1)–H(2)/Å	1.09	1.10	1.11	1.10	–	1.10
C(1)–C(3)/Å	1.54	1.52	1.53	1.72	–	1.71
C(1)–H(11)/Å	1.10	1.13	1.09	1.09	–	1.08
C(3)–C(1)–Nb–Cl/°	331	237	114	317	–	121
Energy/kJ mol^{-1}	1	0	1	0	–	21

elongated C–C bond lengths in Table 4 are a direct consequence of this poor overlap, but should not, in isolation, be interpreted as evidence of strong agostic interactions, as similar elongation occurs in the optimised structure of ethane under similar constraints. We are confident, however, that the relative energies of the different rotamers under these conditions are meaningful for comparative purposes, and the fact that this constraint leads to a stabilisation of rotamer A indicates that the instability of the C–C σ orbitals in cyclopropane is the dominant factor leading to the observed structure of **2a**.

Before leaving this section, we note that an alternative explanation for the elongation of the C–C bond could be made based on *cis*-interactions between the C–C orbitals and those involved in the bonding between the metal and the alkyne. Similar interactions have been noted previously between co-ordinated CO and an adjacent alkyne.[57] However, we regard this type of interaction as highly unlikely because of the geometrical arrangement of the ligands in **2a**. In well-defined examples of this type of '*cis* interaction', the alkyne is oriented parallel to the π-acceptor CO orbital,[57] whereas in **2a** the alkyne is coplanar with the *trans* pyrazolyl group, and sits in the pseudo-symmetry plane of the complex.

Turning to the cyclopentyl system, a comparison of the total energies for L = Tp^{Me2} and L = $Tp^{5\text{-}Me}$ indicates that, in marked contrast to the cyclopropyl system, the steric bulk does play a determining role in the rotamer distribution, removal of the pendant methyl groups reversing the relative stabilities of A and B. Rotamer C is also strongly stabilised, and is now very similar in energy to A. In the *i*-Pr system, a significant structural feature of the most stable rotamer (C) is an opening of the Cβ–Cα–Cβ angle to 119°, simultaneously allowing the system to optimise the agostic interaction and allowing the other methyl group to occupy the least sterically hindered position along the wedge. In the cyclic system, a comparable opening of the Cβ–Cα–Cβ angle is not possible due to the constraints of the ring (Scheme 1), and rotamer C therefore is unable to simultaneously optimise both agostic and steric factors. Rotamers A and B, in contrast, are not effected in the same way, as the corresponding angles, (Hα–Cα–Cβ in both cases) are exocyclic. With rotamer C effectively factored out, the cyclopentyl system is left with a choice between A and B. In the former, an electronically favourable β-C–H agostic interaction is offset by the presence of two β carbons in the most sterically hindered sites, while in the latter the steric repulsions are minimised, but at the expense of forming a less favourable α-C–H agostic bond (Scheme 1). The presence of both rotamers in solution (and also their calculated energetic proximity) confirms that the balance between these two factors is a delicate one but, in this case, the steric demand dominates, leading to an excess of rotamer B. We have not performed explicit calculations on the cyclohexyl systems, but we anticipate that the situation will be rather similar to that described for *c*-C_5H_9. The experimental data are certainly consistent with this proposal, indicating a dominant α-C–H agostic (rotamer B) in equilibrium with a minor species which, by analogy, we tentatively assign as rotamer A.

Summary

A detailed survey of the synthesis and properties of a series of cycloalkyl niobium complexes has revealed a rich chemistry which can be understood in terms of equilibria between different agostic rotamers. For the larger ring systems (*c*-C_5H_9 and *c*-C_6H_{11}), a combination of the steric demands of the Tp^{Me2} ligand and the inflexibility of the endocyclic bond angles combine to favour an α-C–H agostic isomer (confirmed by NMR and, for *c*-C_5H_9, X-ray crystallography). In contrast, the cyclopropyl systems show remarkable properties consistent with the presence of an α-C–C agostic bond, a very unusual type of interaction not observed in any of the other alkyl complexes we have studied, either cyclic or acyclic. In this case the equilibrium position is dominated by electronic factors, in particular the instability of the C–C σ orbitals, which makes them more effective two-electron donors than the surrounding C–H bonds which usually dominate in agostic systems.

Acknowledgements

Bruno Donnadieu (acquisition of X-ray data) and Francis Lacassin (high field NMR) are thanked for their skilfull assistance. Profs. P. G. Edwards and R. Poilblanc are thanked for coordinating the SOCRATES-ERASMUS exchange of M. L. C.; J. J. thanks the MENESER for a thesis grant. M. R. acknowledges financial support from the Improving Human Potential Programme, Access to Infrastructures', under contract HPRI-1999-CT-00071 'Access to CESCA and CEPBA Large-Scale Facilities' established between the European Community and CESCA-CEPBA.

References

1 M. Brookhart, M. L. H. Green and L. L. Wong, *Prog. Inorg. Chem.*, 1988, **36**, 1.
2 A. Haaland, W. Scherer, K. Ruud, G. S. McGrady, A. J. Downs and O. Swang, *J. Am. Chem. Soc.*, 1998, **120**, 3762.
3 M. L. H. Green, A. Sella and L. L. Wong, *Organometallics*, 1992, **11**, 2650.
4 (*a*) M. Brookhart, Lincoln, A. F. Volpe Jr. and G. F. Schmidt, *Organometallics*, 1989, **8**, 1212; (*b*) M. Brookhart, D. M. Lincoln, M. A. Bennett and S. Pelling, *J. Am. Chem. Soc.*, 1990, **112**, 2691.
5 D. J. Tempel, L. K. Johnson, R. L. Huff, P. S. White and M. Brookhart, *J. Am. Chem. Soc.*, 2000, **122**, 6686.
6 M. D. Leatherman, S. A. Svejda, L. K. Johnson and M. Brookhart, *J. Am. Chem. Soc.*, 2003, **125**, 3068.
7 N. Carr, L. Mole, A. G. Orpen and J. L. Spencer, *J. Chem. Soc., Dalton Trans.*, 1992, 2653.
8 J. L. Spencer and G. S. Mhinzi, *J. Chem. Soc., Dalton Trans.*, 1995, 3819.
9 H. Urtel, C. Meier, F. Eisenträger, F. Rominger, J. P. Joschek and P. Hofman, *Angew. Chem., Int. Ed.*, 2001, **40**, 781.
10 W. E. Piers and J. E. Bercaw, *J. Am. Chem. Soc.*, 1990, **112**, 9406.
11 H. Krauledat and H. H. Brintzinger, *Angew. Chem.*, 1990, **102**, 1459.
12 M. J. Tanner, M. Brookhart and J. M. DeSimone, *J. Am. Chem. Soc.*, 1997, **119**, 7617.
13 M. Etienne, *Organometallics*, 1994, **13**, 410.
14 M. Etienne, *Coord. Chem. Rev.*, 1996, **156**, 201.
15 M. Etienne, R. Mathieu and B. Donnadieu, *J. Am. Chem. Soc.*, 1997, **119**, 3218.
16 J.-C. Hierso and M. Etienne, *Eur. J. Inorg. Chem.*, 2000, 839.
17 J. Jaffart, R. Mathieu, M. Etienne, J. E. McGrady, O. Eisenstein and F. Maseras, *Chem. Commun.*, 1998, 2011.
18 J. Jaffart, M. Etienne, F. Maseras, J. E. McGrady and O. Eisenstein, *J. Am. Chem. Soc.*, 2001, **123**, 6000.
19 J. Jaffart, M. Etienne, M. Reinhold, J. E. McGrady and F. Maseras, *Chem. Commun.*, 2003, 876.
20 (*a*) M. D. Fryzuk, S. A. Johnson and S. J. Rettig, *J. Am. Chem. Soc.*, 2001, **123**, 1602; (*b*) C. P. Casey, J. A. Tunge, T.-Y. Lee and M. A. Fagan, *J. Am. Chem. Soc.*, 2003, **125**, 2641.
21 R. H. Grubbs and G. W. Coates, *Acc. Chem. Res.*, 1996, **29**, 85.
22 Z. Guo, D. C. Swenson and R. F. Jordan, *Organometallics*, 1994, **13**, 1424.
23 F. Maseras and K. Morokuma, *J. Comput. Chem.*, 1995, **16**, 1170.

24 M. Svensson, S. Humbel, R. D. J. Froese, T. Matsubara, S. Sieber and K. Morokuma, *J. Phys. Chem.*, 1996, **100**, 19357.
25 F. Maseras, *Chem. Commun.*, 2000, 1821.
26 D. Balcells, G. Drudis-Sole, M. Besora, N. Dolker, G. Ujaque, F. Maseras and A. Lledos, *Faraday Discuss.*, 2003, **124**, DOI: 10.1039/211473a.
27 R. H. Crabtree, *Angew. Chem., Int. Ed.*, 1993, **32**, 789.
28 A. Vigalok and D. Milstein, *Acc. Chem. Res.*, 2001, **34**, 798.
29 G. Lanza, I. L. Fragalia and T. J. Marks, *J. Am. Chem. Soc.*, 2000, **122**, 12764.
30 R. Tomaszewski, I. Hyla-Kryspin, C. L. Mayne, A. M. Arif, R. Gleiter and R. D. Ernst, *J. Am. Chem. Soc.*, 1998, **120**, 2960.
31 M. Etienne, F. Biasotto, R. Mathieu and J. L. Templeton, *Organometallics*, 1996, **15**, 1106.
32 A. Altomare, G. Cascarano, G. Giacovazzo, A. Guargliardi, M. C. Burla, G. Polidori and M. Camalli, *J. Appl. Crystallogr.*, 1994, **27**, 435.
33 D. J. Watkin, C. K. Prout, R. J. Carruthers and P. Betteridge, *CRYSTALS Issue 10*; University of Oxford: Oxford, 1996.
34 J. R. Carruthers and D. J. Watkin, *Acta Crystallogr., Sect. A*, 1979, **35**, 698.
35 D. J. Watkin, C. K. Prout and L. J. Pearce, CAMERON, University of Oxford, Oxford, 1996.
36 M. J. Frisch, G. W. Trucks, H. B. Schlegel, G. E. Scuseria, M. A. Robb, J. R. Cheeseman, V. G. Zakrzewski, J. A. Montgomery, R. E. Stratmann Jr., J. C. Burant, S. Dapprich, J. M. Millam, A. D. Daniels, K. N. Kudin, M. C. Strain, O. Farkas, J. Tomasi, V. Barone, M. Cossi, R. Cammi, B. Mennucci, C. Pomelli, C. Adamo, S. Clifford, J. Ochterski, G. A. Petersson, P. Y. Ayala, Q. Cui, K. Morokuma, D. K. Malick, A. D. Rabuck, K. Raghavachari, J. B. Foresman, J. Cioslowski, J. V. Ortiz, B. B. Stefanov, G. Liu, A. Liashenko, P. Piskorz, L. Komaromi, R. Gomperts, R. L. Martin, D. J. Fox, T. Keith, M. A. Al-Laham, C. Y. Peng, A. Nanayakkara, C. Gonzalez, M. Challacombe, P. M. W. Gill, B. Johnson, W. Chen, M. W. Wong, J. L. Andres, C. Gonzalez, M. Head-Gordon, E. S. Replogle and J. A. Pople, Gaussian; Gaussian, Inc.: Pittsburgh, PA, 1998.
37 L. Cucurull-Sanchez, F. Maseras and A. Lledos, *Inorg. Chem. CommUN.*, 2000, **3**, 590.
38 A. D. Becke, *J. Chem. Phys.*, 1993, **98**, 5648.
39 C. Lee, R. G. Parr and W. Yang, *Phys. Rev.*, 1988, **37**, B785.
40 P. J. Hay and W. R. Wadt, *J. Chem. Phys.*, 1985, **82**, 299.
41 W. R. Wadt and P. J. Hay, *J. Chem. Phys.*, 1985, **82**, 284.
42 A. Höllwarth, M. Böhme, S. Dapprich, A. W. Ehlers, A. Gobbi, V. Jonas, K. F. Köhler, R. Stegmann, A. Veldkamp and G. Frenking, *Chem. Phys. Lett.*, 1993, **208**, 237.
43 W. J. Hehre, R. Ditchfield and J. A. Pople, *J. Phys. Chem.*, 1972, **56**, 2257.
44 P. C. Hariharan and J. A. Pople, *Theor. Chim. Acta*, 1973, **28**, 213.
45 A. K. Rappe, C. J. Casewit, K. S. Colwell, W. A. Goddard III and W. M. Skiff, *J. Am. Chem. Soc.*, 1992, **114**, 10024.
46 (*a*) D. D. Wick and W. D. Jones, *Inorg. Chem.*, 1997, **36**, 2723; (*b*) R. A. Periana and R. G. Bergman, *Organometallics*, 1984, **3**, 508–510.
47 H. N. C. Wong, M.-Y. Hon, C.-W. Tse, Y.-C. Yip, J. Tanko and T. Hudlicky, *Chem. Rev.*, 1989, **89**, 165.
48 (*a*) C. P. Schaller, C. P. Cummins and P. T. Wolczanski, *J. Am. Chem. Soc.*, 1996, **118**, 591; (*b*) J. L. Bennet and P. T. Wolczanski, *J. Am. Chem. Soc.*, 1997, **119**, 10696.
49 P. J. Chirik, M. W. Day, J. A. Labinger and J. E. Bercaw, *J. Am. Chem. Soc.*, 1999, **121**, 10308.
50 A. D. Poole, D. N. Williams, A. M. Kenwright, V. C. Gibson, W. Clegg, D. C. R. Hockless and P. A. O'Neil, *Organometallics*, 1993, **12**, 2549.
51 L. J. Guggenberger, P. Meakin and F. N. Tebbe, *J. Am. Chem. Soc.*, 1974, **96**, 5420.
52 H. Yasuda, H. Yamamoto, T. Arai, A. Nakamura, J. Chen, Y. Kai and N. Kasai, *Organometallics*, 1991, **10**, 4058.
53 H. Shanan-Atidi and K. H. Bar-Eli, *J. Phys. Chem.*, 1970, **74**, 961.
54 P. M. Morse, M. D. Spencer, S. R. Wilson and G. S. Girolami, *Organometallics*, 1994, **13**, 1646.
55 K. S. Cook, W. E. Piers, S. J. Rettig and R. McDonald, *Organometallics*, 2000, **19**, 2243.
56 M. D. Fryzuk, T. S. Haddad and S. J. Rettig, *Organometallics*, 1991, **10**, 2026.
57 J. L. Templeton, *Adv. Organomet. Chem.*, 1989, **29**, 1.